Interfacial delamination of double-ceramic-layer thermal barrier coating system

Xueling Fan[a,b], Rong Xu[a], T.J. Wang[a,*]

[a]State Key Laboratory for Strength and Vibration of Mechanical Structures, School of Aerospace Engineering, Xi'an Jiaotong University, Xi'an 710049, China
[b]Department of Mechanical Engineering, Faculty of Science and Technology, Tokyo University of Science, Chiba 278-8510, Japan

Abstract

Thermal barrier coating system (TBCs) must withstand the most demanding high temperature conditions where state-of-the-art top coat material Y_2O_3–stabilized ZrO_2 may undergo significant sintering and phase change. The concept of double-ceramic-layer (DCL) TBCs seems to be an effective way to meet the need for both thermal stability and transformation toughening. In this paper, a virtual crack closure technique based interface element method is introduced to study the mechanics associated with the interfacial delamination of DCL TBCs. The evolution of energy release rate of interfacial delamination is explored for DCL TBCs with various geometrical and material parameters. Analysis of fracture mechanisms of delamination reveals that considering the integrated thermal and mechanical functionalities of coatings an optimal thickness ratio of outer to inner ceramic layers exists, which can be preliminarily evaluated by running numerical calculations of fracture parameters and performing thermal life experiments over a wide range of thickness ratios of outer to inner coating layers. In addition, the influence of separation centered at the interface of two ceramic layers is also examined. It is demonstrated that the local separation between two ceramic layers makes delamination readily to form and propagate at the interface between the inner coating and the underlying layer.
© 2014 Elsevier Ltd and Techna Group S.r.l. All rights reserved.

Keywords: A: Films; B: Failure analysis; C: Fracture; E: Substrates

1. Introduction

The thermal efficiency of gas turbine for power generation relies on the development of heat resistant materials as well as turbine cooling technology and thermal barrier coating system (TBCs). It has been proved that the turbine inlet temperature increase facilitated with the application of TBCs, in conjunction with advanced air-cooling technology, is much greater than that enabled by heat resistant materials development [1,2], which driving researchers to make every effort to pursuit advantaged TBCs [3]. Due to its low thermal conductivity and high environmental durability, Y_2O_3-stabilized ZrO_2 (YSZ) is increasingly used as the thermal resistant material of TBCs on

the surface of metallic parts in the hottest part of gas turbine engines. Further improvement in the energy efficiency of future gas turbine engines makes the surface temperatures of the top coat (TC) and the bond coat (BC) are higher than those in today's conventional TBCs, which may lead to the deterioration of material properties and thus the decreases of efficiency and reliability [1,4]. The state-of-the-art TC material YSZ performs quite well up to current service temperatures. However, at still higher temperatures, the YSZ mainly undergo two significant detrimental changes: sintering and phase change [5,6]. Over long time high temperature operation, YSZ strongly sinters which leads to microstructure changes and increases in the thermal conductivity and Young's modulus, and hence a reduction of the strain tolerance [5]. On the other hand, the phase transition in YSZ is accompanied by an undesirable volume expansion of about 4% and a considerable reduction of thermal cycling life of TBCs [6].

*Corresponding author. Tel.: +86 29 82663318; fax: +86 29 82669044.
E-mail address: wangtj@mail.xjtu.edj.cn (T.J. Wang).

As a consequence, these disadvantaged high temperature properties of YSZ promoted a worldwide search for candidate materials with superior low thermal conductivity, high melting point, resistance to sintering, and long life properties [3]. Over the past decades, various materials have been developed and considered to be the candidate materials for the future coating [1,7]. A detailed overview on the development of new TBCs material systems was given by Clarke and Levi [3]. It has been proved that the coefficients of thermal expansion (CTE) of these promising candidate materials are typically lower than that of YSZ, which results in higher thermal stresses and thus premature failure of TBCs [8]. Previous studies showed that the need for thermal stability seems contradict with the ability of transformation toughening. Since no single material satisfies all requirements for advanced TBCs, the concept of multilayer seems to be an effective way to overcome this shortcoming. Due to its relatively high CTE and high toughness, traditional YSZ layer is coated to the BC layer. Meanwhile, to protect the inner YSZ layer an additional outer layer with high phase stability and low thermal conductivity is coated on the top of traditional YSZ layer. As a result, a double-ceramic-layer (DCL) coating is formed.

Most of investigations focus on the preparation, characterization, and thermal shock resistance of multilayer thin film/substrate system [8–12]. Relatively little effort has been devoted to the mechanisms governing failure of DCL TBCs. Since the DCL TBCs are composed of multilayer materials with obviously different material properties, relatively large thermal stresses can be induced inevitable in the coatings [13,14]. As a result, interfacial delamination forms, which is believed to govern the durability of coating system [15,16]. The final failure of TBCs happens by spallation of coatings when a separation becomes large enough to create a large scale buckle or an edge delamination [17–19]. The delamination failure is driven by the difference between the stored energy of the debonded and adhered systems. This energy is released during the propagation of the delamination at weak interfaces. Therefore, the central scientific and engineering issue for the application of new developed DCL TBCs is to understand the mechanics of interfacial delamination in terms of energy. Lacking detailed knowledge of failure mechanisms will preclude the application of DCL TBCs in practical gas turbine engines.

In this paper, the evolution of interfacial delamination as well as its dominated material and geometrical parameters is explored numerically. Section 2 briefly reviews the interface fracture mechanics and the concept of an interfacial delamination emanating from the root of a long, straight channel crack. In addition, a user defined element technique based finite element method (FEM) is introduced to calculate the strain energy release rate (SERR) for interfacial delamination. In Section 3, the interfacial delamination of a DCL TBCs structure is investigated by analyzing the effects of material and geometrical parameters of an additional outer coating layer. The influence of separation centered at the interface between two coating layers on the evolution of SERR is also analyzed. Finally, some discussions and concluding remarks are presented in Section 4.

2. Statement of the problem

2.1. Bi–material interface crack

In thin film/substrate structures, two dominate failure modes have been investigated extensively, one for cohesive fracture and the other for interfacial delamination [20]. Multiple surface cracking is the common form of cohesive fracture in thin film structure [21–24]. Once the surface cracks grow sufficiently long compare with the film thickness, a steady state is reached where the energy released per unit advance keeps constant and the crack driving force become independent of the surface crack length and initial flaw geometry [25]. In this case, the steady state SERR of the surface channeling crack can be calculated from a two-dimensional (2D) model [26], which provides a simplified solution that is directly relevant to design against fracture. The previous research found that depending on the elastic mismatch and interface roughness delaminations can be triggered at the roots of the surface channeling cracks [27–29]. In this paper, we consider the mechanisms governing the failure of an interfacial delamination emanating from the root of the surface channel crack at each side in the DCL TBCs, as shown in Fig. 1.

Since the interface of different components is usually a low–toughness fracture path, the delamination is assumed to propagate along the interface. As a sequence, the problem must be concerned with mixed mode crack propagation. Dundurs (1969) has observed that the fracture behavior of an interfacial crack depends on only two non-dimensional combinations of the elastic modulus, known as the Dundurs' elastic mismatch parameters α and β. For the studied 2D plane strain problem, the Dundurs' parameters α and β are expressed as

$$\alpha = \frac{\overline{E}_1 - \overline{E}_2}{\overline{E}_1 + \overline{E}_2} \tag{1}$$

$$\beta = \frac{1}{2} \frac{\mu_1(1-2v_2) - \mu_2(1-2v_1)}{\mu_1(1-v_2) + \mu_2(1-v_1)} \tag{2}$$

where $\overline{E}_i = E_i/(1-v_i^2)$, E_i, v_i and $\mu_i (i=1,2)$ are the plane strain modulus, Young's modulus, Poisson's ratio, and shear modulus of the respective materials, respectively. For most problems, α is more important than β. In case of $E_1 = E_2$, we have $\alpha = \beta = 0$, in other words, the material mismatch vanishes, and the problem reduces to the conventional homogeneous isotropic fracture problem.

The singularity at the crack tips along the interface between two dissimilar isotropic materials is of the form ($\frac{1}{2} \pm i\varepsilon$) where the bi–material constant ε is defined as

$$\varepsilon = \frac{1}{2\pi} \ln \frac{1-\beta}{1+\beta} \tag{3}$$

The singular stress, σ, on the interface directly ahead of the crack tip can be written in the following form [30]

$$\sigma_{yy} + i\sigma_{xy} = (K_1 + iK_2)(2\pi r)^{-1/2} r^{i\varepsilon} \tag{4}$$

where $i = \sqrt{-1}$, $r^{i\varepsilon} = \cos(\varepsilon \ln r) + i \sin(\varepsilon \ln r)$ is the so-called oscillatory singularity parameter for bi–material interface
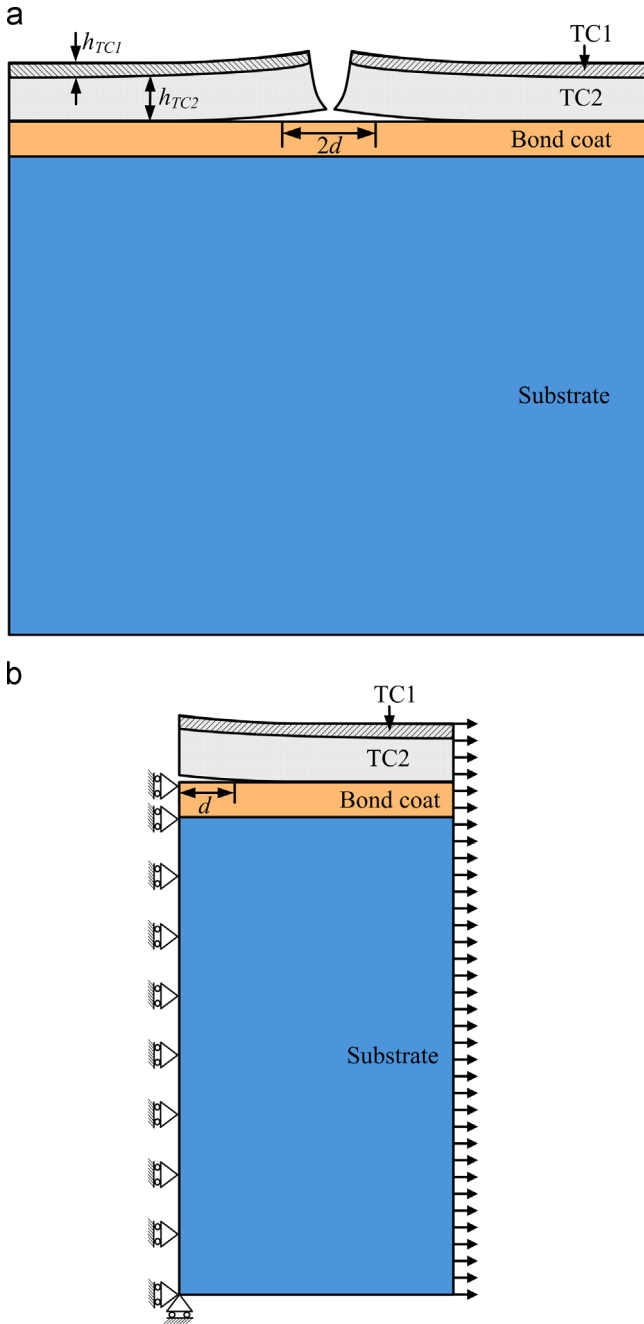
a

b

Fig. 1. (a) Schematic of interfacial delaminations emanating from the root of a surface channel crack in a double-coating-layer thermal barrier coating system (TBCs); and (b) two-dimensional (2D) geometry model of the problem.

crack problem. The interface stress intensity factor (SIF) components K_1 and K_2 play the same role as their well-known counterparts in fracture mechanics for homogeneous, isotropic elastic solids.

And the relative displacement, u, behind the crack tip as

$$\delta_{yy} + i\delta_{xy} = \frac{8}{(1+2i\varepsilon)\cosh(\pi\varepsilon)}\frac{(K_1+iK_2)}{E_*}\left(\frac{r}{2\pi}\right)^{1/2}r^{i\varepsilon} \quad (5)$$

where

$$\frac{1}{E_*} = \frac{1}{2}\left[\frac{1}{\overline{E_1}} + \frac{1}{\overline{E_2}}\right].$$

Based on Irwin's crack closure integral over a virtual crack closure length Δa the SERR, G, for the interface crack can be calculated from Eqs. (4) and (5), as [30]

$$G = \lim_{\Delta a \to 0}\frac{1}{2\Delta a}\int_0^{\Delta a}\boldsymbol{\sigma}(r)\boldsymbol{\delta}(\Delta a - r)\,\mathrm{d}r = \left(\frac{1}{\overline{E_1}} + \frac{1}{\overline{E_2}}\right)\frac{K_1^2 + K_2^2}{2\cosh^2\pi\varepsilon} \quad (6)$$

where Δa is the virtual crack closure length. It can be seen from Eq. (6) the SERR value depends on the elastic mismatch only through ε. Accordingly, the individual SERR components take the form

$$G_I = \lim_{\Delta a \to 0}\frac{1}{2\Delta a}\int_0^{\Delta a}\sigma_{yy}(r)\delta_{yy}(\Delta a - r)\,\mathrm{d}r = \lim_{\Delta a \to 0}\mathrm{Re}\left[\mathbf{C} + \mathbf{D}(\Delta a)^{i\varepsilon}\right] \quad (7)$$

$$G_{II} = \lim_{\Delta a \to 0}\frac{1}{2\Delta a}\int_0^{\Delta a}\sigma_{xy}(r)\delta_{xy}(\Delta a - r)\,\mathrm{d}r = \lim_{\Delta a \to 0}\mathrm{Re}\left[\mathbf{C} - \mathbf{D}(\Delta a)^{i\varepsilon}\right] \quad (8)$$

where the parameters C and D are complex constants [31].

Note that the SERR components depend on the virtual crack closure length Δa due to the presence of oscillatory terms and have no well-defined limits. However, the total SERR value is independent of Δa, and has a definite converged value [32]. The independence of the total SERR value was also reported by others researchers [33,34]. Due to its independence of virtual crack closure length, the evolution of total SERR value is the main concern of the present work.

2.2. Virtual crack closure technique (VCCT) based interface element technique

To predict the delamination advance within interface, the SERR value should be firstly calculated numerically and then compared to the interfacial fracture toughness properties. It has been proved that the SERR value can be calculated numerically by finite element (FE) analysis using the virtual crack closure technique (VCCT), firstly proposed by Rybicki and Kanninen [35]. Based on the formulation of 2D VCCT, for the four-node rectangular element shown in Fig. 2, the SERR value can be approximated as the product of the nodal forces at the crack tip and the nodal displacement opening immediately behind the crack tip

$$G_I = \frac{Y_i(V_j - V_{j'})}{2B\Delta a} \quad (9)$$

$$G_{II} = \frac{X_i(U_j - U_{j'})}{2B\Delta a} \quad (10)$$

where B is the thickness of the body (in case of 2D model, $B=1$), Δa is the length of the elements ahead of the crack tip, and X_i and Y_i are the shear and opening forces at the crack tip (node i), U and V are the shear and opening nodal displacement components along x and y axis, respectively. Node points at upper and lower surface (nodes j and j') have identical coordinates. The new created crack surface is calculated as $\Delta a \times B$.
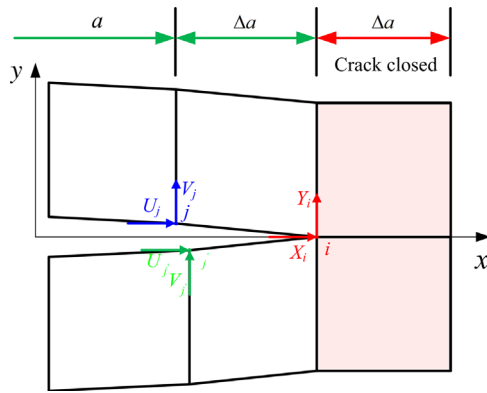
Fig. 2. Virtual crack closure technique (VCCT) for four-node element.

Fig. 3. Definition of VCCT based interface element for 2D four-node element.

For the 2D problem studied, the total SERR can be calculated from the individual mode components as

$$G = G_I + G_{II} \qquad (11)$$

Since there is no additional requirement for the stresses and displacements to fulfill, VCCT can be used with non-singular, linear, FE simulation to get accurate SERR values [34].

To separate the initially bonded nodes, the following general form fracture criterion can be selected to determine the fracture of crack

$$G \geq G_C \qquad (12)$$

where G_C is the critical SERR (fracture toughness), which should be measured via experiments.

In this work, the interfacial delamination in TBCs is numerically studied using the VCCT based interface element technique. The interface element idea follows the methods proposed by Xie and Biggers [36], and Mabson et al. [37], which has been proved to be simple, efficient and robust in crack growth problems.

Fig. 3 shows the definition and node numbering of a typical 2D interface element. Each interface element has five nodes, in which the node pair at the crack tip (N1 and N2) is modeled to calculate the internal forces. A relative stiff spring is allocated between Node 1 and Node 2 to output the internal nodal forces. The node pair immediately behind the crack tip (N3 and N4) is used to extract displacement information. In addition, in order to define the crack growth direction and length the node ahead of the crack tip (N5) is introduced. As a result, two node sets are contained in the interface element: the top set (nodes 1, 3, and 5) and the bottom set (nodes 2 and 4). In practice the top set nodes coincide with the bottom sets before fracture happens. Note that the thickness of interface element is exaggerated for clarity in Fig. 3.

For the studied 2D four-node element, the displacement array of the five-point interface element can be expressed as $\{U_1, V_1, U_2, V_2, U_3, V_3, U_4, V_4, U_5, V_5\}$. Then the nodal forces at the crack tip reads.

$$F_x = K_x(U_1 - U_2), F_y = K_y(V_1 - V_2) \qquad (13)$$

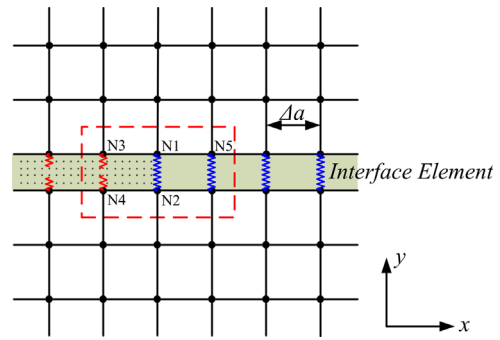where (U_i, V_i) $(i = 1,2)$ are the displacement components for node i referring to the global coordinate system. K_x and K_y are

the stiffness components of the spring allocated between node pair N1 and N2. The stiffness is initially assumed to be a large value and becomes zero once the fracture criterion is satisfied. An empirical validation of the assumption of initial stiffness has been performed in Ref. [36].

Nodes 3 and 4 are introduced to extract displacement information, which do not have contribution to the stiffness matrix of the interface element. Based on the displacement information of Nodes 3 and 4, the shear and opening nodal displacement components behind the crack tip are determined

$$\Delta u = U_3 - U_4, \quad \Delta v = V_3 - V_4 \qquad (14)$$

The crack growth direction is defined by node N5 and node N1, while the crack jump length equals the distance between N5 and N1 and is

$$\Delta a = |U_5 - U_1| \qquad (15)$$

Then, the SERR values can be obtained immediately by substituting Eqs. (13) to (15) into Eqs. (9) to (11). Since the node force and displacement fields are basic information for most of the numerical methods, SERR values can be output directly using the numerical methods such as the FEM in conjunction with the VCCT.

2.3. Finite element model

Numerical calculations are carried out to study the interfacial degradation of DCL TBCs, where the introduced procedure for the VCCT based interface element has been implemented into ABAQUS with its user subroutine UEL. The TBCs structure to be tested is assumed to be sufficiently thick compared to its in-plane geometry such that 2D plane strain model can approximate it. Due to the symmetry of the studied problem, only half of the DCL TBCs structure is modeled with proper boundary conditions imposed (Fig. 1b). User defined elements, which are adopted to characterize the bonding condition of interface, are placed at the interface between BC layer and traditional YSZ layer. For typical FE model of the DCL TBCs structure, non-uniform mesh is adopted with fine mesh constructed around the interface. All layers are treated as isotropic and elastic materials. Their material properties are listed in Table 1(after Refs. [14,38]).

A reference DCL TBCs structure is selected as a benchmark, where the material properties are presented in Table 1 while

Table 1
Material properties of the double-coating-layer thermal barrier coating system.

	Outer ceramic coating (TC1)	Inner ceramic coating (TC2)	Bond coat	Substrate
Young's modulus (GPa)	90	60	200	211
Poisson ratio	0.25	0.1	0.3	0.3

the thicknesses of theTC1, TC2, BC and substrate are assumed to be 50 µm, 250 µm, 100 µm and 3 mm. To evaluate the mechanisms governing the interfacial delamination, different geometries and material properties of outer ceramic layer have been considered, where TC1 thickness varies from 0 to 250 µm, while its Young's modulus varies from 30 to 150 GPa [14,38].

3. Results and discussion

In this section, systematic studies of the influences of geometrical and material properties on interfacial delamination are presented. Note that when the material properties of the outer and inner ceramic layers are assumed to be identical the DCL TBCs structure will reduce to a traditional single-ceramic-layer (SCL) TBCs, where the coating thickness h_f equals to the total coating thickness, $h_{TC1} + h_{TC2}$, of the DCL TBCs (Fig. 1). For comparison, the Young's modulus, Poisson's ratio and stress of the uniform YSZ coating layer of SCL TBCs are represented by E_f, v_f, σ_f, respectively.

3.1. On material parameter effect

Even the smallest increase of turbine inlet temperature can result in considerably large amounts of energy produced, which drives the further improvement of the efficiency for next generation gas turbine engines. As a result, TBCs must be operated at high temperatures, under which coating materials undergo severely sintering phenomenon and the changes of both coating microstructure and material properties [5,6]. Especially, it has been proved that sintering has a significant effect on the mean Young's modulus and hardness of coatings. It is essential to clarify the influence of Young's modulus of outer coating layer on the fracture mechanisms of interfacial delamination. Therefore, numerical calculation of crack driving force has been carried out over a wide range of Young's modulus of outermost ceramic layer. In this section, all of the parameters except for the Young's modulus of outermost layer are held the same with those of the reference DCL TBCs structure.

Due to the well-defined and independence on the virtual crack closure length Δa of total SERR value [32–34], it is first examined as a function of delamination length (Fig. 4). The presented SERR values are normalized by $\sigma_f^2 h_f / \overline{E}_f$, where $\overline{E}_f = E_f / (1 - v_f^2)$ is the plane strain modulus of the uniform YSZ coating of SCL TBCs. The delamination length is normalized by the total coating thickness h_f.

The basic feature of the SERR evolution history is that as delamination length increases a local maximum value will be
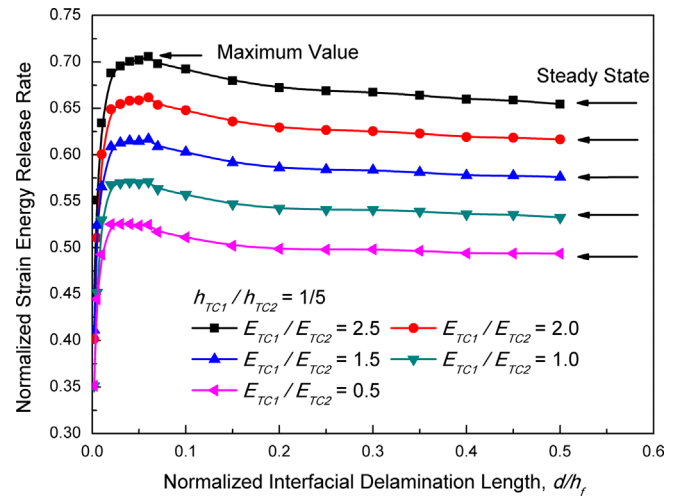

Fig. 4. Normalized strain energy release rate (SERR) for interfacial delamination as the function of Young's modulus ratio of outer to inner coating layers, E_{TC1}/E_{TC2}.

reached for a relatively short crack length (about 6% of the total coating thickness for the studied problem). However, once the delamination propagates sufficient long, less than half of the total coating thickness in this studying, a steady state is reached where the crack driving force becomes independent of the delamination length. As a consequence, the evolution of SERR for an interfacial delamination oscillates instead of a monotonic variation with respect to crack length.

On one hand, the maximum SERR is critical since it determines an interfacial delamination will grow or not. For practical TBCs, the interfacial fracture toughness is constant and determined, an existing separation or delamination grows if the maximum SERR exceeds the fracture toughness, and otherwise, no propagation or coalescence happens. Another key point is that for typical material combination of practical TBCs (the coating is relatively compliant than the underlying layer, that means Dundurs' parameter $\alpha < 0$), the crack driving force approaches zero for very small interfacial delamination ($d/h_f \ll 1$). In other words, in case of $\alpha < 0$, typical TBCs satisfy this condition, a critical size is necessary for the initiation and propagation of interfacial delamination. However, since multiple local separations or delaminations are inevitable even before thermal cycling begins [15,16], the initiation, propagation, linking up and coalescence of small damages can hardly be avoided in practical TBCs. In others film/substrate structure such as microelectronics and stretchable electronics, the substrate can be stiff than the film, which leads to different fracture mechanisms [27,28,39,40].
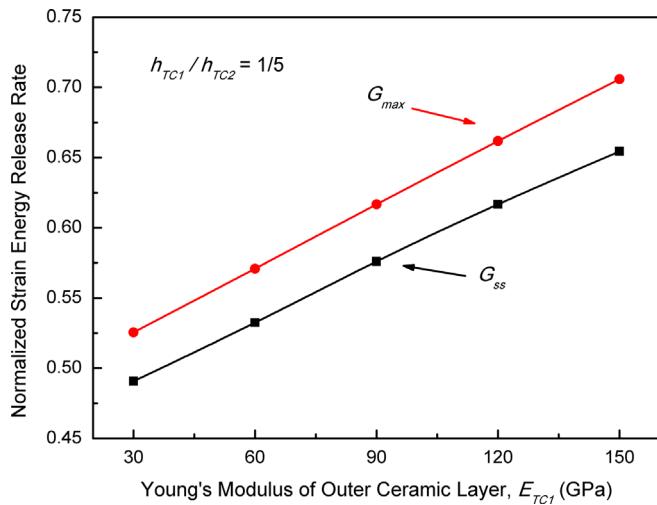
Fig. 5. Variations of the normalized maximum and steady state SERR values presented as the function of the Young's modulus of outer most coating layer, E_{TC1}.

SERR value. In Fig. 6, the normalized SIF components are plotted against the normalized delamination length for different material mismatches of two coating layers, where the SIF components are normalized by $\sigma_f \sqrt{h_f}$.

Analysis of the variation of SIF components indicates that the effects of Young's modulus of TC1 on the SIF components are similar to those of on SERR values. Fig. 6a shows that the opening mode SIF component increases from zero to a maximum value and then decreases to a steady stage value as interfacial delamination propagates. However, instead of an oscillatory variation with respect to crack length the mode II SIF component varies monotonically as the interfacial delamination propagates (Fig. 6b). Therefore, the oscillatory of interfacial crack driving force is mainly caused by the open fracture of coatings. The information of relative amount of mode II to mode I crack driving force at the crack tip is necessary to clarify the mixed mode fracture mechanisms governs the delamination propagation.
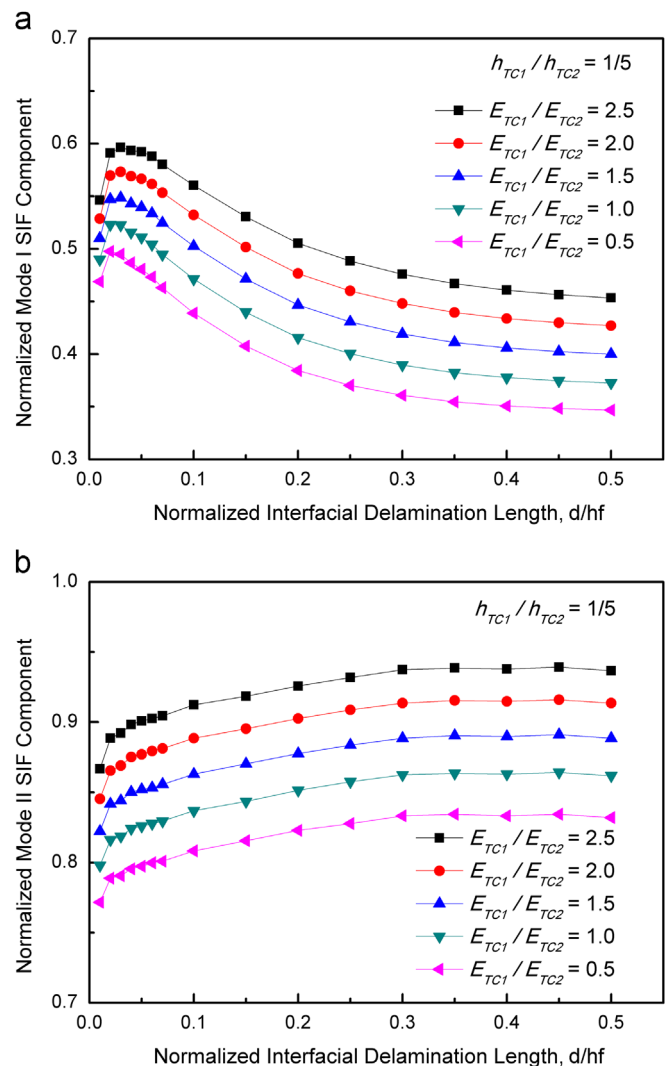
On the other hand, the stead state SERR value is vital to the final failure of TBCs, which is characterized by a large portion of the coating delaminated from the underlying layer. The larger the steady state SERR values the easier a macro-sized separation forms. Moreover, comparing the curves for different material combinations in Fig. 4, we can conclude that depositing a relatively compliant outermost layer can reduce both the maximum and the steady state SERR values. This suggests that better mechanical performance can be achieved by replacing part of the traditional YSZ with relatively compliant ceramic material.

More details can be seen from Fig. 5, where the normalized maximum and steady state SERR values for interfacial delamination are plotted as the function of the Young's modulus of TC1. From Fig. 5, clearly, the elastic mismatch between two ceramic coatings has remarkable effects on the maximum and steady state SERR values. In detail, both the maximum and steady state SERR values increase as the Young's modulus of TC1 increases. Throughout the wide range of elastic moduli, the maximum SERR as well as the steady state SERR displays an approximately linear increase behavior with respect to the Young's modulus of outer ceramic layer. This is caused by the fact that a stiff outermost layer can significantly increase these energy stored in the adhered part, which means more energy will be released by per unit of coating debonding. Hence, we can conclude that due to the sintering-induced stiffening of ceramic coating interfacial delamination can be more easily triggered at elevated temperatures. This can partially explain the premature failure of TBCs under high operation temperature since the elastic modulus of ceramic layer increases with the sintering of coatings at elevated temperatures, more explicitly explain will be left for future studies.

The preceding SERR accounting does not provide any information of the opening and shearing components. The SIF components can be obtained by coupling the Irwin relation with linearity and dimensionality. In this work, the real and imaginary parts of the complex SIF are calculated based on the

Fig. 6. Influence of the Young's modulus ratio of outer to inner coating layers, E_{TC1}/E_{TC2}, on the normalized stress intensity factor (SIF) components for interfacial delamination.

The fracture of delamination should be concerned with mixed mode crack propagation since the interface crack is constrained to evolve along the low-toughness crack path. The material mismatch across the interface as well as non-symmetric geometry and boundary condition induces a mixed mode fracture. One concept, in particular, that plays a central role is the idea of phase angle of mode mix $\Psi = \tan^{-1}(K_2/K_1)$, which measures the relative amount of mode II to mode I crack driving force at the crack tip [25]. In general, the values of total SERR associated with the mode mixity are presented in discussing the interface failure of joined solids. Therefore, the material dependence of mode mixity is also studied in this work. Due to the steady date of SIF components for sufficiently long delamination (Fig. 6), a constant steady state phase angle is expected for relatively long interface cracks and the variation of mode mixity is confined within a small range of delamination length. Therefore, only the steady state mode mixity is plotted with respect to the Young's modulus of TC1 layer (Fig. 7). Observe that the steady state mode mixity strongly depends on the elastic modulus of outer most ceramic layer. In particular, the reduction of steady state mode mixity is approximately proportional to the increase of elastic modulus of TC1 layer. A decrease in the mode mixity suggests that the effect of opening mode becomes more significant, which is undesirable because it may cause relatively large out-of-plane displacement. Regarding the possibility of sintering induced densification in outer most ceramic layer at high temperatures, coating endurance may be reduced significantly, which makes novel microstructure coatings or more efficient candidate materials valuable.

3.2. On geometrical parameter effect

Attention is confined in this section to the effect of relative thickness of two ceramic layers on the SERR values for delamination at the TC2/BC interface (Fig. 8). The presented SERR values in Fig. 8 is again normalized by $\sigma_f^2 h_f / \overline{E}_f$, while the delamination 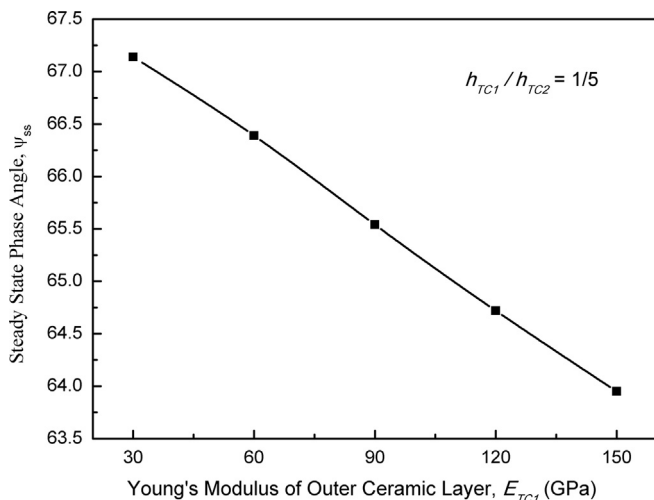length is normalized by the total thickness of two coating layers h_f. Herein, the material properties of TC1 layer are assumed to these presented in Table 1.

As discussed in the previous section, oscillation occurs for all considered situations. Similar to the variation of SERR with respect to the elastic modulus of outer most coating layer, the SERR value approaches to zero as $d/h_f \to 0$, which implies that for very small interface defects the crack driving force will vanish in case of a relative compliant film deposited on a stiffer substrate. As interfacial delamination length increases, a steady state is approached for sufficient long crack. According to Fig. 8, the steady state SERR value increases remarkably with the thickening of stiff outer ceramic layer. Consequently, accompany with its basic function of thermal isolation an additional stiff outer coating layer yields a high risk of coatings debonding as compared to SCL TBCs. This suggests that the need for additional coating layer to avoid severely sintering and phase transformation contradicts with the need for lower interfacial crack driving force. As a result, an optimal thickness of outer coating layer may exist, which points to important challenges and directions for the future work.

Again, we focus on the variations of the maximum and the steady state SERR values. We can notice that both the maximum and the steady state SERR values increase with the thickening of outer most ceramic layer. Further, it seems that the increases of the maximum and the steady state SERR values are approximately linear with respect to the normalized thickness of outer coating layer. As stated by Dai et al. [41] based on their experimental observations, a critical thickness ratio of outer to inner layers exists for DCL TBCs, above which the thermal life is dramatically decreased and below which the thermal life is relatively long. Fig. 9 will play some role in extending the application of thermal life data of DCL TBCs, such as these presented in Ref. [41]. In other words, Fig. 9 provides a preliminary evaluation method for the determining of interfacial toughness of a multilayer coating TBCs. The purpose can be achieved by performing the following steps. First, thermal cycling tests of DCL TBCs
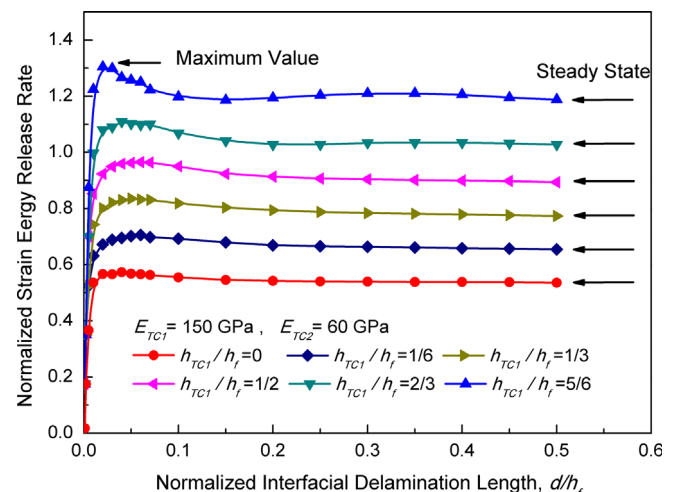

Fig. 7. Variation of steady state phase angle of mode mix as a function of Young's modulus of outermost ceramic layer thickness.

Fig. 8. Normalized SERR plotted as the function of the normalized delamination length d/h_f for several normalized outermost ceramic layer thicknesses, h_{TC1}/h_f.
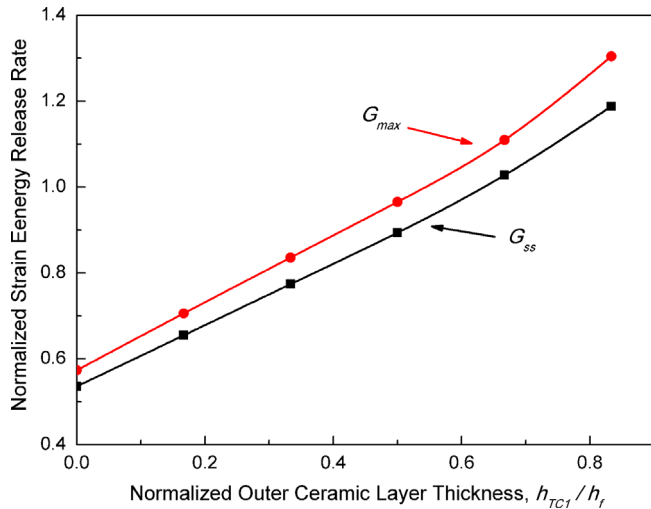
Fig. 9. Variations of the normalized maximum and steady state SERR values as a function of the normalized thickness of outermost ceramic layer, h_{TC1}/h_f.

with different thickness ratios of outer to inner layer should be performed. Then, identify the experimental data of the thermal life in the numerically predicted plot of SERR against outer layer thickness, such as Fig. 9, and draw a vertical line from the critical thickness ratio where thermal life jump is observed. Then, a horizontal line can be drawn from the intersection of the SERR curve with the vertical line. As a result, the y–axis intercept can be obtained, which is believed to correspond to the normalized interfacial toughness of the studied DCL TBCs. Consequently, the key outcome of Fig. 9 is that the interfacial bonding strength of a DCL TBCs can be evaluated by comparing the experimentally observed critical outermost coating thickness, which separates the thermal life into higher and lower regions, with the numerically predicted SERR values against coating thickness. In addition, notes can be made as to whether the propagation of interfacial delamination is stable or unstable after running numerical calculations of SERR and performing burner rig test of thermal life over a wide range of outer layer coating thicknesses. On the other hand, after experimentally determining the interfacial toughness of a DCL TBCs it is also possible to preliminary evaluate the optimal thickness of outer most coating layer based on the variation of SERR with respect to the relative thickness of two coating layers.

3.3. On interfacial separation effect

Due to the inherent weakness of interface, local separations or defects at interfaces are inevitable in TBCs [42]. Analysis of experimental observations reveals that final failure of TBCs is results of the initiation, propagation, linking up and coalescence of small, isolated regions of damage [15,16], which makes it meaningful to study the effect of local separations on the interfacial delamination. Due to their significant effects on the interfacial fracture behavior of TBCs, as discussed in above sections, the evolutions of maximum and stead-state SERR values are examined to illustrate the influence of local

separation (Fig. 10), where a single delamination of size w is assumed to be centered at the TC1/TC2 interface.

Fig. 10 shows the normalized SERR values for interfacial delamination at TC2/BC interface as a function of separation size at the interface of TC1 and TC2. These results clearly show the significant effect of defect at theTC1/TC2 interface on the crack driving force of delamination at the TC2/BC interface. As evident in both of the curves in Fig. 10, increase of the maximum and stead state SERR values for the interfacial delamination are nonlinear as the defect size increases and a suddenly rising up occurs once the separation size becomes sufficiently large (about one millimeter, three times of total coating thickness in this work). Large scale buckling may occur due to possibly unstable propagation of delamination associated with out-of-surface stresses. Moreover, compared to that of local maximum SERR value, the effect of defect on the steady state SERR values is more significant. This is straightforward since the maximum value occurs for very short interfacial delamination, which means the distance between the separation and the delamination is so large that the influence of defect is relatively insignificant. However, as the distance decreases between two delaminations the influence on the maximum SERR values become significant and have to be considered. Since the maximum SERR value and the stead state SERR value play decisive roles in the initiation and propagation of delamination, respectively, the existing of defects makes delaminations readily to form and coalescence with others. However, the complexity of failure mechanisms makes it difficult to quantitatively describe this relationship, and further experimental data is needed to determine the most appropriate physically based mathematical description.

4. Conclusion

The demands and promises of still high efficiencies and to operate at much higher temperatures of most advantage gas
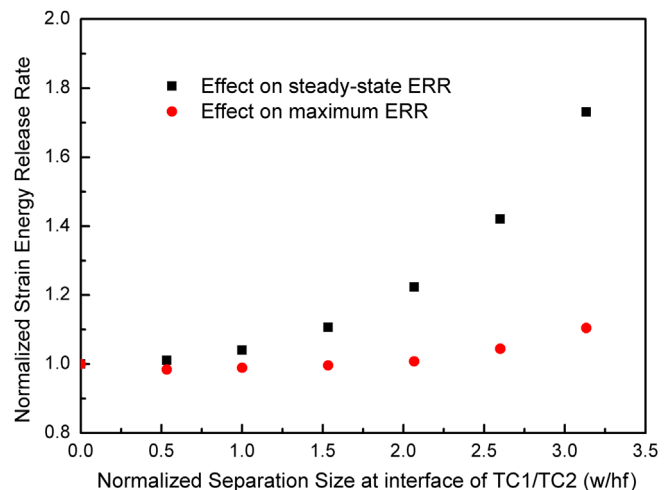

Fig. 10. Influence of defect at TC1/TC2 interface on the normalized SERR for interfacial delamination at TC2/BC interface. SERR is normalized by the SERR results of $E_{TC1}/E_{TC2}=1.5$ in Fig. 4 and $h_{TC1}/h_{TC2}=0.2$ in Fig. 8.

turbines, are driving new thermal barrier coating system (TBCs) based on coating materials development and innovative multi-layer evolving system. Various candidate materials have been explored but it seems that the requirement for thermal stability contradict with the ability of transformation toughening, which motivates the concept of multi-layer TBCs. However, relatively little effort has been devoted to understanding of the mechanisms governing the failure of multi-ceramic-layer TBCs.

In this paper, a virtual crack closure technique (VCCT) based interface element method is used to study the interfacial delamination of a double-ceramic-layer (DCL) TBCs. Numerical analysis is performed by implementing the interface element with the commercial finite element analysis software ABAQUS with its user subroutine technique UEL. The variation of strain energy release rate (SERR) for interfacial delamination is examined. In addition, the influences of material and geometrical parameters on the interfacial crack driving force are studied. Some main conclusions are summarized as follows.

(1) The evolution of SERR for interfacial delamination oscillates with respect to crack length, which leads to the existences of local maximum and stead state SERR values. Both the maximum and steady state SERR values increase with the thickening of outer most coating layer.
(2) Approximately linear increases of the maximum and the steady state SERR values are observed with respect to the relative elastic modulus of outer to inner layers. It is believed that interfacial delamination can be more easily triggered at elevated temperatures due to the sintering-induced stiffening of outermost ceramic coating.
(3) The optimal thickness ratio of outer to inner coating layers can be preliminarily evaluated by combining the experimental thermal life data with the numerically predicted SERR values against outer most coating layer thickness.
(4) Defect at the interface of two ceramic layers has significant effect on the interfacial delamination at the interface of coatings and bond coat. In detail, the increases of the maximum and stead state SERR values for the interfacial delamination are nonlinear as the defect size increases and an abrupt rising up appears once the separation length increases to a critical size of millimeter magnitude.

Acknowledgments

References

[1] D.R. Clarke, M. Oechsner, N.P. Padture, Thermal-barrier coatings for more efficient gas-turbine engines, MRS Bull. 37 (2012) 891–898.
[2] N.P. Padture, M. Gell, E.H. Jordan, Thermal barrier coatings for gas-turbine engine applications, Science 296 (2002) 280–284.
[3] D.R. Clarke, C.G. Levi, Materials design for the next generation thermal barrier coatings, Annu. Rev. Mater. Res. 33 (2003) 383–417.
[4] J.R. Nicholls, Advances in coating design for high-performance gas turbines, MRS Bull. 28 (2003) 659–670.
[5] R. Vaßen, F. Traeger, D. Stöver, New thermal barrier coatings based on pyrochlore/YSZ double-layer systems, Int. J. Appl. Ceram. Technol. 1 (2004) 351–361.
[6] J.R. Brandon, R. Taylor, Phase stability of zirconia-based thermal barrier coatings part I. Zirconia-yttria alloys, Surf. Coat. Technol. 46 (1991) 75–90.
[7] R. Vaßen, X.Q. Cao, F. Tietz, D. Basu, D. Stöver, Zirconates as new materials for thermal barrier coatings, J. Am. Ceram. Soc. 83 (2000) 2023–2028.
[8] X.Q. Cao, R. Vaßen, F. Tietz, D. Stöver, New double-ceramic-layer thermal barrier coatings based on zirconia-rare earth composite oxides, J. Eur. Ceram. Soc. 26 (2006) 247–251.
[9] M. Han, J.H. Huang, S.H. Chen, Behavior and mechanism of the stress buffer effect of the inside ceramic layer to the top ceramic layer in a double-ceramic-layer thermal barrier coating, Ceram. Int. 40 (2014) 2901–2914.
[10] M. Han, G.D. Zhou, J.H. Huang, S.H. Chen, Optimization selection of the thermal conductivity of the top ceramic layer in the double-ceramic-layer thermal barrier coatings based on the finite element analysis of thermal insulation, Surf. Coat. Technol. 240 (2014) 320–326.
[11] X. Feng, Y. Huang, A.J. Rosakis, Multi-layer thin films/substrate system subjected to non-uniform misfit strains, Int. J. Solids Struct. 45 (2008) 3688–3698.
[12] M.A. Brown, A.J. Rosakis, X. Feng, Y. Huang, E. Ustundag, Thin film/substrate systems featuring arbitrary film thickness and misfit strain distributions. Part II: experimental validation of the non-local stress/curvature relations, Int. J. Solids Struct. 44 (2007) 1755–1767.
[13] X. Feng, Y. Huang, A.J. Rosakis, Stresses in a multilayer thin film/substrate system subjected to nonuniform temperature, J. Appl. Mech.–Trans. ASME 75 (2008) 021022.
[14] L. Wang, Y. Wang, W.Q. Zhang, X.G. Sun, J.Q. He, Z.Y. Pan, C.H. Wang, Finite element simulation of stress distribution and development in 8YSZ and double-ceramic-layer La$_2$Zr$_2$O$_7$/8YSZ thermal barrier coatings during thermal shock, Appl. Surf. Sci. 258 (2012) 3540–3551.
[15] V.K. Tolpygo, D.R. Clarke, K.S. Murphy, Evaluation of interface degradation during cyclic oxidation of EB–PVD thermal barrier coatings and correlation with TGO luminescence, Surf. Coat. Technol. 188–189 (2004) 62–70.
[16] B. Heeg, V.K. Tolpygo, D.R. Clarke, Damage evolution in thermal barrier coatings with thermal cycling, J. Am. Ceram. Soc. 94 (2011) S112–S119.
[17] P.K. Wright, A.G. Evans, Mechanisms governing the performance of thermal barrier coatings, Curr. Opin. Solid State Mater. Sci. 4 (1999) 255–265.
[18] T.Q. Lu, W.X. Zhang, T.J. Wang, The surface effect on the strain energy release rate of buckling delamination in thin film-substrate systems, Int. J. Eng. Sci. 49 (2011) 967–975.
[19] Z.X. Chen, K. Zhou, X.H. Lu, Y.C. Lam, A review on the mechanical methods for evaluating coating adhesion, Acta Mech. (2013) 1–22.
[20] A.G. Evans, J.W. Hutchinson, The mechanics of coating delamination in thermal gradients, Surf. Coat. Technol. 201 (2007) 7905–7916.
[21] X.L. Fan, W.X. Zhang, T.J. Wang, G.W. Liu, J.H. Zhang, Investigation on periodic cracking of elastic film/substrate system by the extended finite element method, Appl. Surf. Sci. 257 (2011) 6718–6724.
[22] W.X. Zhang, X.L. Fan, T.J. Wang, The surface cracking behavior in air plasma sprayed thermal barrier coating system incorporating interface roughness effect, Appl. Surf. Sci. 258 (2011) 811–817.
[23] Z.X. Chen, K. Zhou, X.H. Lu, Y.C. Lam, A review on the mechanical methods for evaluating coating adhesion, Acta Mater. (2013) 1–22.
[24] X.L. Fan, W.X. Zhang, T.J. Wang, Q. Sun, The effect of thermally grown oxide on multiple surface cracking in air plasma sprayed thermal barrier coating system, Surf. Coat. Technol. 208 (2012) 7–13.
[25] J.W. Hutchinson, Z. Suo, Mixed-mode cracking in layered materials, Adv. Appl. Mech. 29 (1992) 63–191.

[26] J.L. Beuth Jr, Cracking of thin bonded films in residual tension, Int. J. Solids Struct. 29 (1992) 1657–1675.

[27] H.X. Mei, Y.Y. Pang, R. Huang, Influence of interfacial delamination on channel cracking of elastic thin films, Int. J. Fract. 148 (2007) 331–342.

[28] X.L. Fan, R. Xu, W.X. Zhang, T.J. Wang, Effect of periodic surface cracks on the interfacial fracture of thermal barrier coating system, Appl. Surf. Sci. 258 (2012) 9816–9823.

[29] R. Xu, X.L. Fan, W.X. Zhang, Y. Song, T.J. Wang, Effects of geometrical and material parameters of top and bond coats on the interfacial fracture in thermal barrier coating system, Mater. Des. 47 (2013) 566–574.

[30] M.Y. He, J.W. Hutchinson, Crack deflection at an interface between dissimilar elastic materials, Int. J. Solids Struct. 25 (1989) 1053–1067.

[31] I.S. Raju, J.H. Crews, M.A. Aminpour, Convergence of strain energy release rate components for edge-delaminated composite laminates, Eng. Fract. Mech. 30 (1988) 383–396.

[32] C.T. Sun, C.J Jih, On strain energy release rates for interfacial cracks in bi–material media, Eng. Fract. Mech. 28 (1987) 13–20.

[33] A. Agrawal, A.M. Karlsson, Obtaining mode mixity for a bimaterial interface crack using the virtual crack closure technique, Int. J. Fract. 141 (2006) 75–98.

[34] R. Krueger, K. Shivakumar, I.S. Raju, Fracturemechanics analyses for interface crack problems a review, in: Proceedings of the 54th AIAA/ASME/ASCE/AHS/ASC Structures, Structural Dynamics and Materials Conference (AIAA), Boston, MA, US, 2013, pp. 2013–1476.

[35] E.F. Rybicki, M.F. Kanninen, A finite element calculation of stress intensity factors by a modified crack closure integral, Eng. Fract. Mech. 9 (1977) 931–938.

[36] D. Xie, S.B. Biggers, Progressive crack growth analysis using interface element based on the virtual crack closure technique, Finite Elem. Anal. Des. 42 (2006) 977–984.

[37] G. Mabson, L. Deobald, B. Dopker, Fracture interface elements, Mil Handbook 17, , 2003.

[38] H.F. Chen, Y. Liu, Y.F. Gao, S.Y. Tao, H.J. Luo, Design, preparation, and characterization of graded $YSZ/La_2Zr_2O_7$thermal barrier coatings, J. Am. Ceram. Soc. 93 (2010) 1732–1740.

[39] K. Zhou, L.M. Keer, Q.J. Wang, Analysis of hard coatings on a substrate containing inhomogeneities, J. Mech. Mater. Struct. 6 (2011) 627–639.

[40] T. Ye, Z. Suo, A.G. Evans, Thin film cracking and the roles of substrate and interface, Int. J. Solids Struct. 29 (1992) 2639–2648.

[41] H. Dai, X.H. Zhong, J.Y. Li, Y.F. Zhang, J. Meng, X.Q. Cao, Thermal stability of double-ceramic-layer thermal barrier coatings with various coating thickness, Mater. Sci. Eng. A 433 (2007) 1–7.

[42] X.L. Fan, W. Jiang, J.G. Li, T. Suo, T.J. Wang, R. Xu, Numerical study on the interfacial delamination of thermal barrier coatings with multiple separations, Surf. Coat. Technol. 244 (2014) 117–122.